

GT2011-46354

## Integrated Combustor – Turbine Design for Improved Aerothermal Performance : Effect of Dilution Air Control

A. M. Basol, K. Regina, A. I. Kalfas<sup>1</sup>, R. S. Abhari  
LEC, Laboratory for Energy Conversion  
Department of Mechanical and Process Engineering  
ETH Zurich  
Zurich, Switzerland  
Email: basola@lec.mavt.ethz.ch

### ABSTRACT

*The effect of dilution air control in a combustor on the heat load distribution of an axial turbine with non-axisymmetric endwall profiling is examined. Endwall profiling is a more common design feature in new engine types, due to the effectiveness of the endwall profiling in reducing secondary flows, and their associated losses.*

*In the present work, the effect of dilution air control is examined by using two different circumferentially non-uniform hot-streak shapes; the two cases differ in their spanwise extents either side of the stator, and therefore represent different approaches for dilution air control. This numerical study details the impact of these two different strategies for dilution air control on the rotor blade heat load distribution. The inlet boundary conditions simulate the experiment that is conducted in the axial research turbine facility “LISA” at ETH Zurich. A circumferential non-uniformity in the spanwise migration pattern of the hot streak inside the stator is observed. Even though this circumferential non-uniformity in the spanwise migration is alleviated by the non-axisymmetric endwall profiling, the two hot-streak cases result in considerably different heat load distributions on the rotor blade, emphasizing the importance of the integrated combustor – turbine approach. Finally, the implications for dilution air control on the liner are discussed for the realization of the simulated hot streak shapes in a real combustor.*

### NOMENCLATURE

P pressure  
T temperature

#### Greek

$\Delta$  difference  
 $\mu$  viscosity

#### Abbreviations

CFD computational fluid dynamics  
FENT Fast Response Entropy Probe  
HP high pressure  
HS hot streak  
OpenMp Open Multi-Processing  
PV passage vortex  
RANS Reynolds Averaged Navier Stokes  
TLV tip leakage vortex  
TVD Total Variation Diminishing  
y+ dimensionless number showing the wall resolution

#### Subscripts

aw adiabatic wall  
circ circumferentially mass averaged  
rel relative state  
0 stagnation condition  
1 turbine inlet

---

<sup>1</sup>Current address: Aristotle University of Thessaloniki, Greece

## INTRODUCTION

In gas turbines the temperature field at the combustor outlet exhibits strong non-uniformities. As the non-uniformities convect downstream the relatively high temperature regions termed hot streaks locally increase the incident heat load on downstream components, and can lead to failures at critical regions due to overheating. Apart from this impact on heat loads, hot streaks have a distinct migration pattern, generating secondary flows within rotating blade rows and thereby also losses. Given their profound impact, hot streaks have been investigated both experimentally and numerically in a number of previous studies.

One of the first experimental studies was undertaken by Butler et al. [1] in a single-stage, low speed rig with a circular hot streak introduced from a tube upstream of the stator. Here it was shown that the hot streaks result in preferential heating on the pressure side of the rotor blades due to the high relative flow angle; this is known as the Kerrebrock-Mikolajczak effect [2] The hot streak segregation observed by Butler et al. [2] has also been investigated numerically. However, the two dimensional studies of Rai and Dring [3] and Krouthen and Giles [4] did not correctly capture the heat load distribution observed in the experiment. On the other hand, the good match with experiments in three-dimensional simulations by Dorney et al. [5] and Takahashi et al. [6] emphasized the importance of three-dimensional effects on hot streak migration.

Due to environmental regulations that place limits on NO<sub>x</sub> levels, designers are forced to limit the peak temperature levels without decreasing the mean turbine entry temperature, in order to keep thermal efficiency at high levels. This has led to more uniform radial temperature profiles resulting in an increase in heat loads on endwalls and on the rotor blade tip.

The radial temperature profile at the combustor outlet has a primary effect on the spanwise heat load distribution on downstream components. From design point of view, turbine cooling is carried out using this one dimensional temperature boundary condition. In addition, blade rows downstream of the first stage stator, especially the rotor row, are also influenced by the cooling air ejected from the stator and by the spanwise migration pattern in the stator itself, which re-positions and re-shapes the hot streak inside the passage. Although it might have a more secondary effect on the spanwise heat load distribution, at these elevated temperature levels it can be important to consider this re-positioning and re-shaping when designing the turbine. By using the migration pattern inside the stator and coupling the temperature distribution at combustor outlet accordingly in an integrated combustor –

turbine approach, the incident heat load on the rotor blade can be considerably reduced.

The migration characteristics of hot streaks inside the first stage stator have been investigated by An et al. [7] for six different clocking positions. Depending on the clocking position of the circular hot streak relative to the stator, a considerable change in the position and shape of the hot streak downstream of the stator has been observed. The spanwise migration pattern of a circular hot streak inside the stator with axisymmetric endwalls has been studied in a previous numerical work [8], revealing the effect of the aerodynamics of the first stage stator on the hot streak migration pattern through the stage. It has been shown that due to the opposite spanwise migration patterns on either side of the stator, the circumferential temperature gradients at the combustor outlet affect the spanwise heat load distribution on the downstream rows. Clocking the hot streak even by less than 1° towards the pressure side of the stator, the heat load on the rotor blade tip can be considerably reduced. Taking into account the trend towards more flat temperature profiles at the combustor exit, shaping of the hot streak in circumferential direction close to the endwalls can be quite effective for the heat load distribution on the turbine blade tips.

However, to make use of the fuel injector – stator clocking in that regard necessitates an equal number of fuel injectors and stators, which is rarely the case in real engines. Because of this limitation, instead of clocking of the fuel injectors, the dilution air holes on the liner can be considered to shape the hot streak close to the endwalls according to the migration pattern in the stage.

Due to its effectiveness in reducing secondary flows, endwall profiling is increasingly becoming a more common design feature in modern gas turbines [9-11]. Especially in low aspect ratio blades such as in first stage stators, the asymmetry at the endwalls can have a considerable effect on the migration pattern along the whole span. Consequently, the temperature non-uniformity that is convected through the stator can be exposed to a considerable change of its shape and position.

In the present work, the convection pattern of a circumferentially non-uniform hot streak shape in a highly loaded axial turbine is numerically investigated. For this study the inlet boundary conditions are taken from recent measurements in the one-and-a-half stage axial research turbine facility “LISA” at ETH Zurich, where the first stage stator has non-axisymmetric endwall profiling. First the simulation results are compared with the measurements both in terms of the mixing of the hot streak and the losses that are generated. Using a particle tracking tool in conjunction with the unsteady flow data of the simulations, the migration pattern in the stator is investigated and the effect of the endwall profiles on this migration pattern is explored. Then in the light of this information the experimentally generated hot streak shape is rotated around its center which would

correspond to a different positioning of the dilution holes on the liner. Both hot streak shapes have been compared in terms of the heat load distribution on the rotor blade. Finally, the implications of this study for the combustor dilution air control are discussed.

## EXPERIMENTAL METHOD

The experimental investigation of hot streak migration was performed in the axial research turbine "LISA" in the Laboratory for Energy Conversion at ETH Zurich. The one-and-1/2 stage unshrouded turbine is representative of a high work, cooled turbine. Further details of the experimental facility are presented by Behr et al. [12] For the current experimental study on hot streaks, an inlet temperature distortion generator was added to the existing configuration. The generator has at its outlet, a non-axisymmetric shape with a larger radial extent along one axis compared to the other axis; this asymmetry simulates the effect of non-uniform positioning of dilution air holes on the combustor liner in real engines.

Measurements were carried out at stationary planes upstream and downstream of each row of the first stage. The layout of the measurement planes and also the location of the hot streak generator are shown in Figure 1.

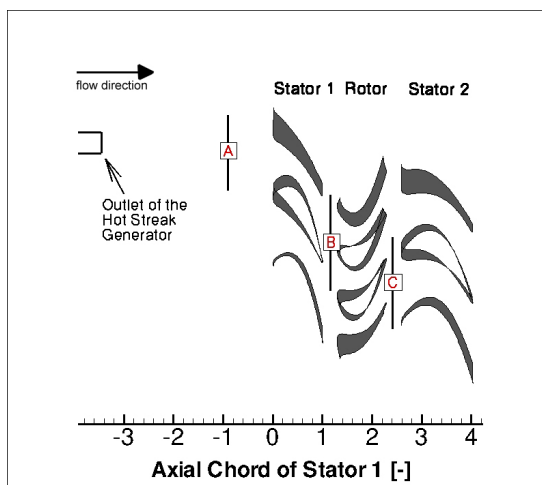


**Figure 1.** Layout of the turbine showing the location of the hot streak generator. The three measurement planes A,B and C are also shown.

The peak-to-mean temperature ratio of the hot streak at the measurement plane A is 1.16. The temperature ratio is a critical parameter having a primary influence on the hot streak migration pattern in rotating blade rows due to its direct effect on the secondary flow generation. There is a big variety in the temperature ratios used in combustors depending on the design

field of application. Compared to the study of Povey et al. [13], this ratio is in the range observed in modern annular combustors. The peak temperature is approximately positioned at mid-span and mid passage between the two stator blades. The circumferential extent of the hot streak is chosen such that the hot streak is confined within one stator pitch.

Time-resolved pressure, temperature and flow angle measurements have been carried out using the in-house fast response entropy probe "FENT". Complete details of this probe can be found in Mansour et al. [14]. Time averaged flow field measurements are carried out with five hole probe.

## Geometry

The high work turbine consists of two stationary rows having 36 stator blades each and a rotating row composed of 54 rotor blades. First stage stator has a constant exit angle design and stacked radially along its leading edge. The profile shape, with a large leading edge radius and large profile thickness was chosen to model the shape of an internally cooled high-pressure gas turbine vane. Among these three rows only the first stator has non-axisymmetric end wall profiling whereas the other two rows have conventional axisymmetric endwalls. More details of about the non-axisymmetric endwall design are discussed by Germain et al. [9] and flow field measurements are presented by Schuepbach et al. [10]

Within the rotor the flow is redirected by an average turning angle of  $\epsilon=122^\circ$  at a moderate rotational speed of 2700 rpm which results in a mean loading coefficient of  $\Psi=2.36$ . The rotor has a flat tip with a tip clearance height of 1% of the rotor blade span. A summary of the profile parameters can be found in Table 1. Further details of the design are presented by Behr et al. [12]

**Table 1.** Characteristic geometry and performance parameters of the 1<sup>st</sup> stage of the turbine at the design operating point

	Stator 1	Rotor
Number of blades	36	54
Inlet flow angle	0°	54°
Outlet flow angle	73°	-67°
Solidity	1.27	1.41
Aspect ratio	0.87	1.17
Exit Mach number	0.54	0.50
Reynolds number based on true chord and blade relative exit velocity	$7.1 \times 10^5$	$3.8 \times 10^5$

## NUMERICAL METHOD

### Solver

The in-house CFD code "MULTI3" used in this study is an unsteady compressible RANS solver. The solution method is based on an explicit, finite-volume, node-based, Ni-Lax-Wendroff time-marching algorithm developed by Ni [15]. The discretization is second order both in time and space. To prevent high frequency oscillations and to capture shock waves, a combined second and fourth order numerical smoothing is added. For closure of the RANS equations a two equation Wilcox  $k-\omega$  turbulence model [16] is implemented in its low Reynolds number form. The implementation is based on an upwind TVD scheme for the discretization of the convective fluxes in the turbulence model. To speed-up the convergence, a local time-stepping approach is used for steady simulations, and dual time-stepping for time resolved simulations.

The solver has been parallelized using OpenMP and can run parallel in a shared memory architecture. More information on the solver can be found in Burdet et al. [17]

### Mesh

In this numerical study only the first stage of the turbine is modeled and due to the integer stator rotor ratio only 1/18th of the whole annulus is used. Thus, the computational domain consists of two rows with 2 stators and 3 rotor blades. The mesh of the geometry has been generated using the in-house multi-block grid generator MESHBOUND [18]. The mesh is first generated with axisymmetric endwalls and then in a second step the non-axisymmetric endwall profiles are introduced into the mesh with the aid of Fourier coefficients [19]. As a last step, the mesh is smoothed at the connection points of the blocks using a Laplacian operator [20]. In Figure 2 the surface mesh is shown with the profiled endwalls. The  $y^+$  values for the rotor row are summarized in Table 2.

**Table 2.** Information about the mesh size and wall resolution

$\overline{y^+}$ rotor PS	$\overline{y^+}$ rotor SS	$\overline{y^+}$ rotor tip	Total number of cells (million)
2.7	2.4	3.4	3.3

### Particle Tracking Tool

The in-house particle tracking tool "UNS-TRACK" has been developed as a post-processing tool for the purpose of studying the hot streak migration pattern in the turbine stage. The snapshots at different physical times are written out by the

flow solver, and are then used as an input for the particle tracking tool. The time marching of the particles is based on the 3rd order Adams Bashforth method. Since the tool is not integrated into the solver, the time interval between the flow field data at adjacent time steps can be larger than the CFL limit for particles at the solid boundaries and may result in some particles penetrating into the wall. To prevent this unphysical situation, the wall perpendicular components of the velocity vectors of the particles inside wall boundary layers are omitted, and thus prevented from penetrating into solid walls. Information about the validation of the particle tracking tool can be found in Basol et al. [8]

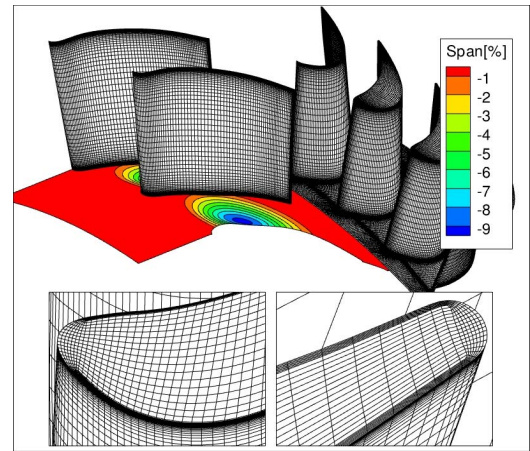


**Figure 2.** Surface meshes on the stator and rotor blades and the rotor hub. Along the stator hub, the contours show the geometry of the non-axisymmetric endwall profiling. The inserts show details of the mesh at the leading and trailing edges of the rotor tip.

## VALIDATION OF FLOW SOLVER

### Boundary Conditions

For validation of the present numerical method, the experimentally measured hot streak shape at plane A (Figure 1) has been imposed as an inlet boundary condition and the computed temperature distribution downstream of the rotor (plane C) is compared with the measurements. The imposed total temperature distribution is shown in Figure 3 together with the total pressure deviation relative to the mean total pressure. The wake of the hot streak generator can be identified with the deficit in total pressure.

The yaw and pitch angles at the inlet of the computational domain are also derived from the measurements upstream of the stator. There are slight deviations from the axial direction both circumferentially and radially due to a distortion of the flow by the temperature distortion generator.

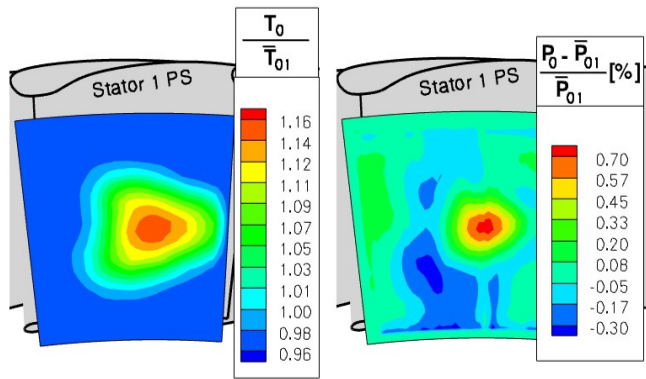


**Figure 3.** Measured total temperature (left) and total pressure deviation (right) at plane A. These measured data are used as the inlet boundary conditions for the solver.

The turbulence intensity measured at plane A is also imposed as an inlet boundary condition in order to be able to capture the turbulent mixing between the hot streak and the free stream. The peak turbulent intensity is in excess of 10% in the core of the hot streak. To calculate the eddy dissipation downstream of the hot streak generator, a turbulent length scale is needed which is estimated assuming a fully developed pipe flow inside the generator. The convection of the eddy viscosity imposed at the stator inlet through the stage is shown in Figure 4.

The blade walls are treated as no-slip, adiabatic surfaces, and a sliding mesh approach is used to transfer information between the computational domains of the two blade rows.

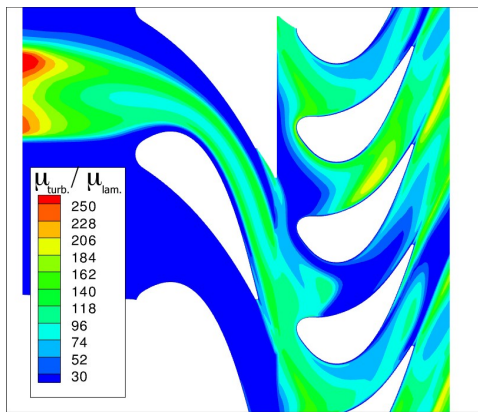


**Figure 4.** Convection of the eddy viscosity imposed at the stator inlet generated as a result of the interaction of the hot streak generator with the free stream

## Convergence

For the unsteady simulations a dual time stepping approach has been used. The temporal resolution is 100 time steps per three rotor blade passing periods. The convergence is checked by monitoring the pressure at the periodic faces between the rows. Starting from a steady solution a periodic solution is achieved after 500 time steps.

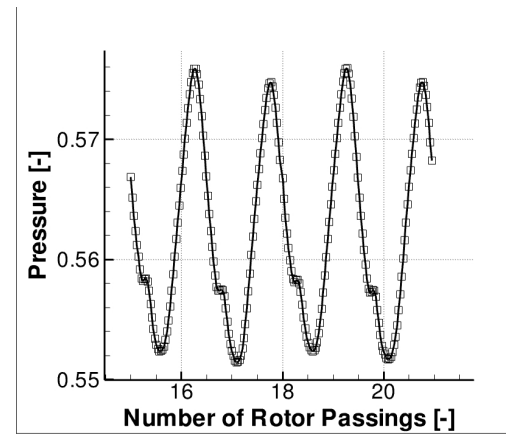


**Figure 5.** Variation of static pressure at the inlet of the rotor domain at midspan. The variation is periodic due to the stator - rotor interaction

## Rotor Exit Flow Field

In order to gain better insight about the hot streak migration inside the rotor passage, the measurements carried out downstream of the rotor row (plane C) in the stationary frame of reference are transformed into the rotor relative frame of reference. In Figure 6 the measured time averaged relative total temperature distribution at rotor outlet is shown with the prediction of the solver. It is evident that, there is a good qualitative match between the measured and predicted temperature distributions in the rotor passage. The peak temperatures are closer to the rotor pressure side, which shows the preferential migration of hot streak towards the pressure side. The temperature value at the core of the hot streak is predicted to be 1.5% higher than the measurement, which indicates that the turbulent mixing between the hot streak and the free stream is under-predicted in the simulation. Both measurement and prediction show a similar spanwise migration pattern of the hot streak on each side of the rotor blade. This migration is a result of the secondary flow pattern inside the passage. The hot streak spreads radially along the pressure side of the rotor blade and migrates over the tip, as seen in both measurement and prediction. The main loss structures are visible as regions with a low relative total temperature.

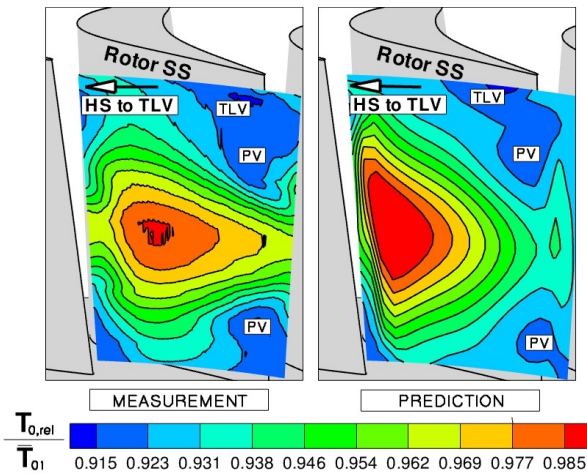


**Figure 6.** Time averaged relative total temperature distributions downstream of the rotor (rotor relative frame of reference)

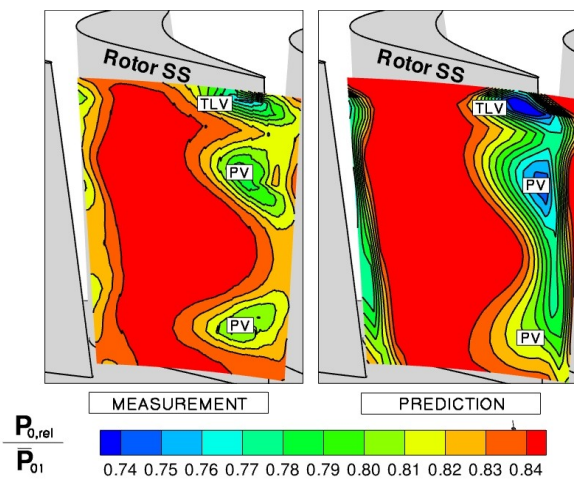


**Figure 7.** Time averaged relative total pressure distributions downstream of the rotor (rotor relative frame of reference)

In Figure 7 the time averaged relative total pressure distributions downstream of the rotor row are shown both for the measurements and for the simulation results. The three distinct loss structures, the tip leakage vortex and the upper and lower passage vortices are clearly seen in both measurement and prediction. For the reliability of the results of this numerical work, the accurate prediction of the tip leakage vortex is of major importance, because this vortex focuses on the heat load on the rotor blade tip that is greatly influenced by the tip leakage vortex. In that regard, there is a good qualitative match in the size and position of the tip

leakage vortex and other loss cores. However, as a general trend, the pressure levels in the loss cores are under-predicted in the simulation, which might be due to the underpredicted turbulent eddy viscosity. As a result the shear between the loss cores and the free stream is underpredicted, reducing the mixing of the loss cores. That's why the loss cores in the simulation have a more distinct footprint than in the experiment at the plane of interest. The largest difference is in the core of the tip leakage vortex, where the predicted pressure level is 4% less than the measurement.

## RESULTS

### Particle Tracking Study

The pattern of the hot streak's migration onto the rotor blade tip and the role of the stator in modulating this pattern are next investigated. The particle tracking tool, that is described above, is used for this analysis. In the analysis 2400 particles are distributed uniformly at the stator inlet over an area that is 1.30 times wider than the stator pitch and that covers about 35% of the blade span. In Figure 8 this area is bordered by a black line. As the particles are convected through the computational domain, the rotor blades are simultaneously rotated in a manner that is similar to a sliding mesh approach. Several particle releases with the same number of particles and from the same positions are carried out over a time interval equal to one rotor blade passing. In this way a time averaged flow pattern of the particles migration to the rotor blade tip can be obtained. After the particles are convected through the domain, the particles that migrated to the rotor blade tip are detected and their origins at the inlet plane are then located. In Figure 8, the initial distribution of the particles that are released at the stator inlet and subsequently migrate to the rotor tip is shown. It can be seen that there is substantial circumferential non-uniformity in the distribution of the particles. Particles released close to the stator suction side can migrate to the rotor tip even though they start close to the midspan of the stator. On the other hand, among all particles released close to the pressure side of the stator, only particles that are initially higher than 87% span convect to the rotor tip.

In order to investigate the effect of the stator on this migration pattern, the distribution of the same particles shown in Figure 8 are next examined at the stator outlet plane in Figure 9. The particles are colored according to the change in their spanwise positions relative to their radii at their initial positions at the stator inlet plane. A positive change in the spanwise position indicates a migration of the particle towards the tip endwall. On the other hand, a negative change indicates a migration towards the hub endwall. It is evident from the pattern seen in Figure 9, that particles closer to the suction side of the stator have a positive radial flow reaching up to 4% of

the span of the stator. On the other hand, particles closer to the stator pressure side have an opposite radial flow reaching of up to -4% of the span of the stator. The circumferentially increased uniformity in the distribution of the particles compared to the distribution at the stator inlet plane shown in Figure 8, reveals the importance of the spanwise migration patterns inside the stator on the hot streak migration pattern. The still existing non-uniformity indicates other aspects of the flow that are not uniform in circumferential direction.

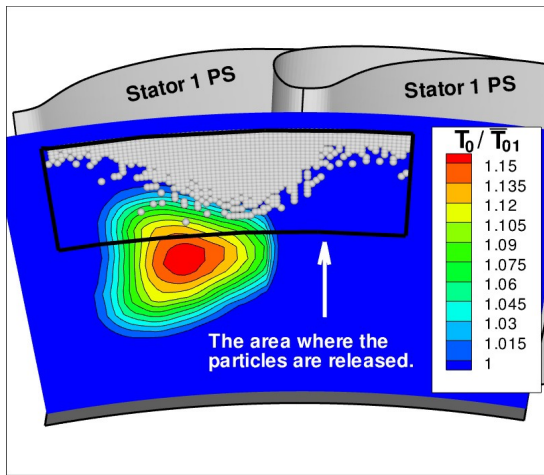


**Figure 8.** Distribution of the particles migrating to the rotor blade tip among all released from the area shown by the black curve upstream of the stator with *non-axisymmetric* endwalls. The temperature distribution at the stator inlet plane is shown in the background contour.

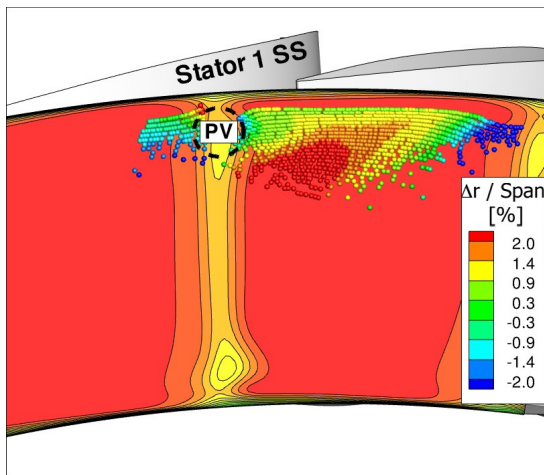


**Figure 9.** Distribution of the same particles shown in Figure 8 at the stator outlet plane. The particles are colored according to the change in their spanwise positions relative to the radii of their starting positions in the stator inlet plane. The total pressure distribution is shown in the background contours.

### Effect of the Endwall Profiling on the Migration Pattern

To evaluate the effect of the endwall profiling on the migration pattern in the turbine stage, the same particle tracking study has been carried out with the same inlet boundary conditions and turbine geometry but the first stage stator has been replaced with another one having axisymmetric endwalls. This stator with the axisymmetric endwalls and the previous one with the non-axisymmetric endwalls have the same blade profiles but only differ at the shape of the endwalls. Detailed flow field measurements of these two stators have been carried out by Schuepbach et al. [10]

Figure 10 shows the distribution of the particles migrating to the rotor blade tip released from the same area upstream of the stator 1 with axisymmetric endwall profiles. Also in this case a circumferentially non-uniform distribution pattern is observed, showing an increased spanwise migration pattern for the particles close to the suction side of the stator. Generally, the two distributions shown in Figures 8 and 10, have the same characteristics. To be able to compare these distribution patterns more accurately, the number of particles migrating to the rotor blade tip from each circumferential position has been plotted for both of the cases. As shown in Figure 11, the main difference between the two curves is in the distribution of the particles close to the pressure sides of the stator. In the stator with the non-axisymmetric endwall profiling more particles managed to migrate to the rotor blade tip compared to the one with the axisymmetric endwalls. So the circumferential non-uniformity in the spanwise migration pattern seems to be weakened by the effect of the non-axisymmetric endwalls.

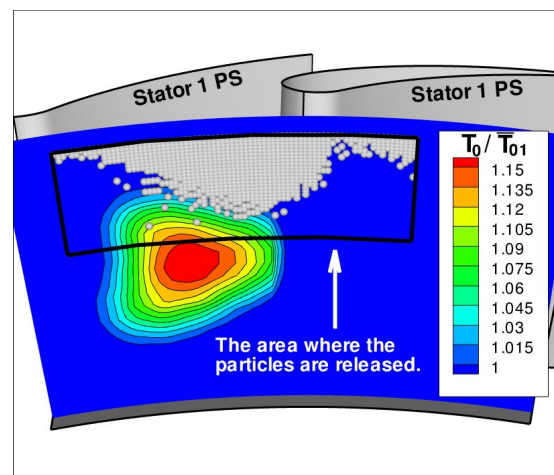


**Figure 10.** Distribution of the particles migrating to the rotor blade tip among all released from the area shown by the black curve upstream of the stator with *axisymmetric* endwalls. The temperature distribution at the stator inlet plane is shown in the background contour.

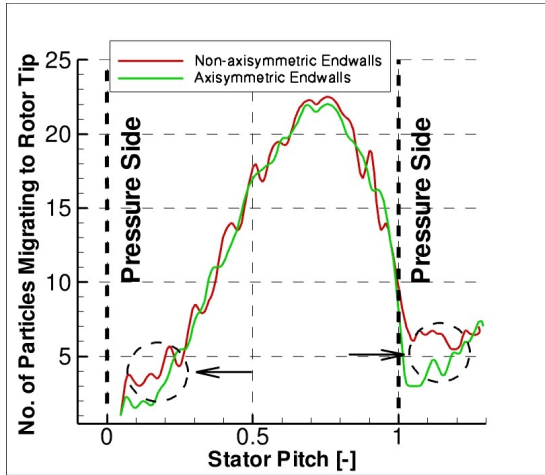


**Figure 11.** Comparison of the distribution of the number of the particles migrating to the rotor blade tip released from each circumferential position upstream of the stators with and without non-axisymmetric endwall profiling. (The stator leading edge is at zero stator pitch.)

To investigate the effect of the non-axisymmetric endwall profiling on the streamline pattern inside the stator, streamlines are released at 90% span where the effect of the endwall profiling is expected to be pronounced. In Figure 12, the radial positions of two streamlines released at 90% span from each side of the stators (both with and without endwall profiling) have been plotted with respect to the axial distance from the inlet of the domain. In the stator with axisymmetric endwalls, the streamline close to the suction side shows increase and decrease in its spanwise position depending on the axial position. However, in total the streamline ends up at a higher spanwise position downstream of the stator relative to its position at the stator inlet, whereas the streamline close to the pressure side shows a continuous drop in its spanwise position. So there is a considerable difference in the spanwise positions of the streamlines at their endpoints downstream of the stator even though they have started from the same spanwise position upstream of the stator. On the other hand, inside the stator with non-axisymmetric endwalls, both of the streamlines released from each side of the stator show first a radial migration towards the tip and then move towards the hub. There is also a difference in the spanwise positions of the streamlines at their endpoints downstream of the stator but not as much as the difference in the radial positions of the streamlines inside the stator with axisymmetric endwalls. This clearly shows the effect of the endwall profiling unifying the spanwise migration pattern at each side of the stator. Because of this reason more particles released from the pressure side of the stator might migrate to the rotor blade tip.

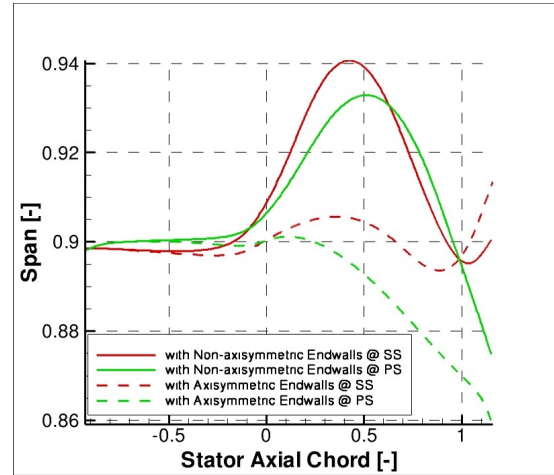


**Figure 12.** Variation in the radial positions of the streamlines with respect to the axial chord of the stators released from either side of the stators with and without endwall profiling (Stator leading edge is at zero axial chord)

### Hot Streak Shaping

Based on the migration pattern to the rotor blade tip that is observed above, a hot streak shaping is next conducted and its impact on the rotor blade heat load is investigated. For this study the experimentally measured hot streak shape is taken as the baseline case. For the other hot streak shape to compare, the baseline hot streak is rotated around its axis, which would correspond to the clocking of the dilution holes on the liner towards the pressure side of the stator. The temperature distributions at the stator inlet plane for the two cases are shown in Figure 13. Both hot streak shapes are imposed upstream of the stators with and without non-axisymmetric endwalls. In this manner the effect of the hot streak shaping on the rotor blade heat load distribution will be evaluated using stators with two different endwall shapes.

To enhance the effect of the hot streak on the rotor blade tip, in the numerical study both hot streak shapes are displaced by 10% in spanwise direction relative to the experimentally measured test case. An axial inflow and uniform total pressure distribution are used as inlet boundary conditions. That's why this study involves only the shaping of the temperature profiles and excludes the effect of non-uniform total pressure fields on the heat load distribution. A uniform turbulent intensity of 10% is used for both of the cases as well.

The circumferentially mass averaged temperature profiles of the two hot streak shapes are shown in Figure 14. Both profiles are identical indicating that the distribution of spanwise heat addition is the same in these two cases.

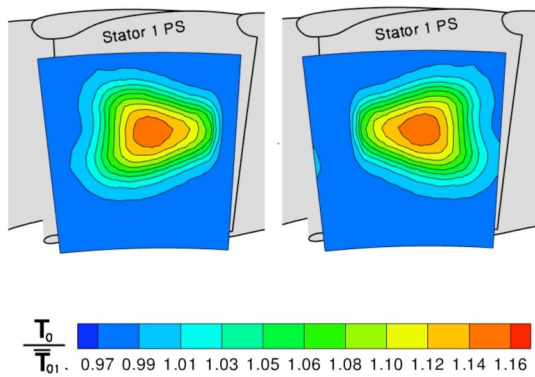


**Figure 13.** Total temperature distribution at the stator inlet plane for baseline(left) and rotated(right) hot streak cases

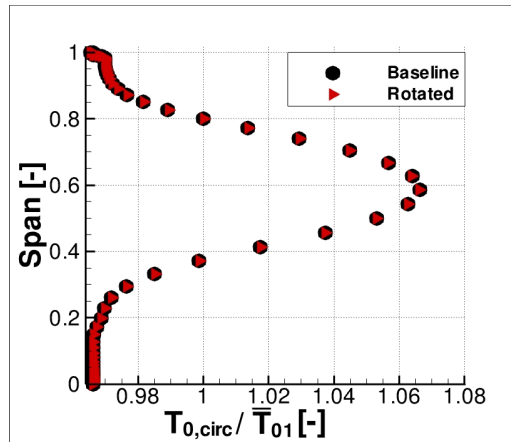


**Figure 14.** Circumferentially mass averaged total temperature profiles at the inlet of the stator for both hot streak shapes

### Change in the Rotor Blade Adiabatic Wall Temperatures

Time resolved, multi-row simulations for the two cases yielded solutions from which the time averaged heat load distributions on the rotor blades can be determined. In Figures 15 and 16 the percentage differences in the time averaged adiabatic wall temperatures on the rotor blade due to the rotation of the hot streak shape are shown. The results in Figure 15 are obtained using the stator with non-axisymmetric endwall profiling and the ones in Figure 16 with axisymmetric endwalls at the stator. In both Figures regions with negative values indicate a decrease in adiabatic wall temperatures imposing the baseline hot streak case as it is in comparison to the rotated one. A 0.5 % change in the temperature level would correspond to a 9 K change in the adiabatic wall temperatures under real engine conditions, with a mean turbine inlet temperature of 1800 K. In both Figures zones

with a reduction of heat load are located along the midspan and at the tip closer to the leading edge of the blade. Closer to the trailing edge of the blade tip the reductions in temperature get smaller in magnitude. In both Figures there are also regions where an increase in the adiabatic wall temperatures is observed. These are mainly on the pressure side of the blade in form of two bands extending from the leading edge to the trailing edge. The baseline hot streak case leads to higher temperature levels at these regions of the blade. Having the spanwise longer side of the hot streak close to the pressure side of the stator, the baseline hot streak spreads in radial direction more relative to the rotated hot streak and leads to increased temperature levels on the rotor blade close to the hub and tip of the rotor blade. On the other hand, this spanwise expansion reduces the peak temperature levels around the midspan which reflects as a reduction in temperature levels around the midspan of the blade. This spanwise expansion of the hot streak at the pressure side of the stator has been previously observed by An et al. [7]

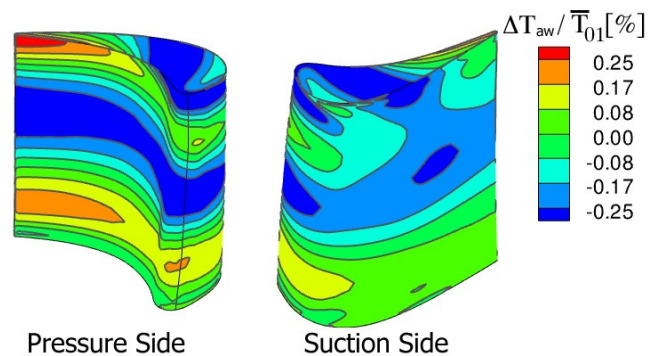


**Figure 15.** Difference in the rotor blade adiabatic wall temperatures between the two hot streak shapes imposed upstream of the stator with *non-axisymmetric* endwall profiling ( $\Delta T_{aw} = T_{aw, baseline} - T_{aw, rotated}$ )

Apart from the main features both Figures 15 and 16 share, there are also slight differences in the change in the adiabatic wall temperatures due to the effect of the endwall profiling. The main differences between these two Figures are close to the tip of the rotor blade. The point of the temperature rise close to the trailing edge of the blade in Figure 15 is slightly higher than the one observed in Figure 16. Also the region with a reduction in temperature covers a smaller area at the blade tip in Figure 15 in comparison to the area in Figure 16. From that point of view the hot streak shaping study seems to be more effective with the axisymmetric endwall shapes. The effect of the non-axisymmetric endwalls unifying the opposite spanwise migration pattern inside stator indicates that

slightly lower circumferential temperature gradient close to the endwall is required.

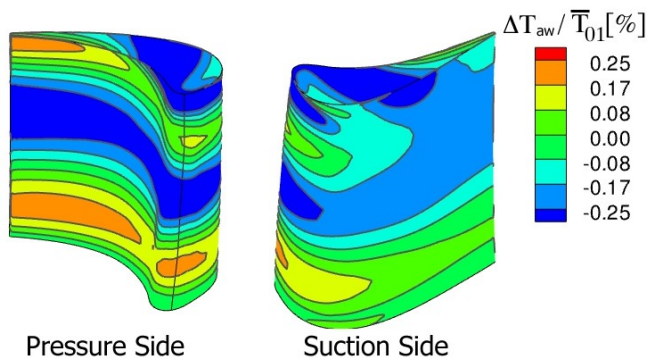


**Figure 16.** Difference in the rotor blade adiabatic wall temperatures between the two hot streak shapes imposed upstream of the stator with *axisymmetric* endwall profiling ( $\Delta T_{aw} = T_{aw, baseline} - T_{aw, rotated}$ )

### Impact on the Combustor Design

There is a trend in combustor design towards having more uniform radial temperature profiles at the combustor outlet, thereby increasing the incident heat load on the endwalls. As one of the critical parts of the turbine, the rotor blade tip is exposed to higher heat loads, it is instructive to assess the design implications of circumferential hot streak shaping close to the endwalls.

The heat load downstream of the stator is affected by the combustor outlet temperature profile and by the flow field of the stator itself as well. In addition to the downstream effects of the cooling air injected at the stator surface, the spanwise migration pattern inside the stator also has a considerable effect on the temperature distribution downstream of the stator. This characteristic of the flow field means that the circumferential temperature distribution is an important design parameter to be considered in managing the spanwise heat load distribution on the rotor blade. Even though using non-axisymmetric endwalls seems to alleviate the opposite spanwise migration pattern on opposite sides of the stator, still the circumferential temperature gradients are highly effective on the spanwise heat load distribution on the downstream rows.

In modern annular combustors it is seldom the case to have equal number of fuel injectors and stators, and the circumferential temperature non-uniformities at mid span are rather low. So there is little degree of freedom for the shaping of the temperature field at the midspan using the fuel injector – stator clocking approach. However, the observed potential in reducing rotor tip heat load by circumferentially shaping the

hot streak close to the endwalls can be realized by proper positioning of the dilution holes on the combustor liner. In this way even though there is an unequal number of fuel injectors and stators, a periodic temperature pattern can be formed close to the endwalls in order to exploit of the previously discussed migration pattern. This circumferential non-uniformity in the temperature distribution can be realized by the non-uniformity either in the distribution or in the size of the dilution holes on the combustor liner.

### CONCLUSIONS

In the present work, the effect of a combustor’s dilution air control on the spanwise heat load distribution of the rotor blade positioned downstream of a stator that has non-axisymmetric endwall profiling is examined. Two circumferentially non-uniform hot-streak shapes are used which differ in their spanwise extents either side of the stator and therefore represent two different approaches for dilution air control in a combustor. Even though alleviated by the endwall profiling, the circumferential non-uniformity in the spanwise migration pattern of the hot streak, which is shown to be majorly influenced by the flow field of the stator, leads for the baseline hot streak case (having a larger radial extent close to the pressure side of the stator) to reduced adiabatic wall temperatures reaching up to 9 K in real engine conditions. The results emphasize the importance of the circumferential hot streak shaping on the aerothermal performance of the turbine which can be realized by the dilution air control on the liner in real combustors.

### ACKNOWLEDGEMENTS

The authors would like to thank to MTU Aero Engines GmbH for the permission of using their endwall profiling design. Contribution of Prof. Ndaona Chokani is also greatly appreciated.

### REFERENCES

- [1] Butler, T. L., Sharma, O. P., Joslyn, H. D., and Dring, R. P., 1989. “Redistribution of an Inlet Temperature Distortion in an Axial Flow Turbine Stage”. *Journal of Propulsion and Power*, 5(1), pp. 64–71.
- [2] Kerrebrock, J., and Mikolajczak, A., 1970. “Intra-Stator Transport of Rotor Wakes and Its Effect on Compressor Performance”. *Journal of Engineering for Power*, 92(4), pp. 359–369.
- [3] Rai, M., and Dring, R., 1990. “Navier-Stokes Analysis of the Redistribution of Inlet Temperature Distortions in a Turbine”. *Journal of Propulsion and Power*, 6, pp. 276–282.

- [4] Krouthen, B., and Giles, M., 1990. "Numerical Investigation of Hot Streaks in Turbines". *Journal of Propulsion and Power*, 6(6), pp. 769–776
- [5] Dorney, D., Davis, R., Edwards, D., and Madavan, N., 1992. "Unsteady Analysis of Hot Streak Migration in a Turbine Stage". *Journal of Propulsion and Power*, 8(2), pp. 520–529.
- [6] Takahashi, R., and Ni, R.-H., 1996. "Unsteady Hot Streak Migration Through a 1 -Stage Turbine". AIAA Paper No.96-2796.
- [7] An, B., Liu, J., and Jiang, H., 2009. "Numerical Investigation on Unsteady Effects of Hot Streak on Flow and Heat Transfer in a Turbine Stage", *Journal of Turbomachinery*, 131(3), 031015
- [8] Basol, A. M., Jenny, P., Mohamed, I., Kalfas, A.I., Abhari, R. S., 2010. "Hot Streak Migration in a Turbine Stage :Integrated Design to Improve Aerothermal Performance", ASME GT2010-23556.
- [9] Germain, T., Nagel, M., Raab, I., Schuepbach, P., Abhari, R. S., 2008. "Improving Efficiency of a High Work Turbine Using Non-Axisymmetric Endwalls: Part I—Endwall Design and Performance", ASME GT2008-50469
- [10] Schuepbach, P., Abhari, R.S., Rose, M.G., Germain, T., Raab, I., Gier, J., 2008. "Improving Efficiency of a High Work Turbine Using Non-Axisymmetric Endwalls: Part II—Time-Resolved Flow Physics", ASME GT2008-50470
- [11] Jenny, P., Abhari, R.S., Rose, M.G., Brettschneider, M., Gier, J., 2011. "A Low Pressure Turbine with Profiled End Walls and Purge Flow Operating with a Pressure Side Bubble", ASME GT2011-46309
- [12] Behr, T., Kalfas, A., and Abhari, R., 2007. "Unsteady Flow Physics and Performance of a One-and-1/2-Stage Unshrouded High Work Turbine". *Journal of Turbomachinery*, 129(2), pp. 348-359
- [13] T. Povey, I. Q., 2009. "Developments in Hot-Streak Simulators for Turbine Testing", *Journal of Turbomachinery*, 131(3), 031009
- [14] Mansour, M., Chokani, N., Kalfas, A., and Abhari, R., 2008. "Impact of Time-Resolved Entropy Measurements on a One-And-1/2-Stage Axial Turbine Performance", ASME GT2008-50807.
- [15] Ni, R., 1981. "A Multiple Grid Scheme for Solving the Euler Equations", *AIAA J.*, 20(3), pp. 1565–1571.
- [16] Liu, F., Zheng, X., 1994. "Staggered Finite Volume Scheme for Solving Cascade Flow with a  $k-\omega$  Turbulence Model", *AIAA J.*, 32(8), pp. 1589-1597
- [17] Burdet, A., and Abhari, R., 2007. "Three-Dimensional Flow Prediction and Improvement of Holes Arrangement of a Film-Cooled Turbine Blade Using a Feature-Based Jet Model". *Journal of Turbomachinery*, 129(2), pp. 258-268
- [18] Mischo, B., Behr, T., and Abhari, R., 2008. "Flow Physics and Profiling of Recessed Blade Tips: Impact on Performance and Heat Load". *Journal of Turbomachinery*, 130. 021008
- [19] Buehler, N., 2006. Investigation of Effects of Blade Hub Fillets on Secondary Flows in an Axial Turbine Using CFD, Master Thesis, ETH Zurich
- [20] Blazek, J., 2005. *Computational Fluid Dynamics: Principles and Applications*, Elsevier